IEEE Access
Multidisciplinary ⁝ Rapid Review ⁝ Open Access Journal

Received September 28, 2019, accepted October 16, 2019, date of publication October 23, 2019, date of current version November 5, 2019.

Digital Object Identifier 10.1109/ACCESS.2019.2949097

A Bi-Level Linearized Dispatching Model of Active Distribution Network With Multi-Stakeholder Participation Based on Analytical Target Cascading

PULIANG DU[1], ZHONG CHEN[1], YANXI CHEN[1], ZIWEN MA[1], AND HONGEN DING[2]
[1]School of Electrical Engineering, Southeast University, Nanjing 210096, China
[2]State Grid Jiangsu Electric Power Company Electric Power Research Institute, Suzhou 230088, China

Corresponding author: Zhong Chen (chenzhong_seu@163.com)

This work was supported by the State Grid Jiangsu Science and Technology Project under Grant SGTYHT/17-JS-199.

ABSTRACT This paper addresses a linearized interactive dispatching model developed between active distribution network (ADN) and virtual micro-grid (VMG). To make such concept, a bi-level framework is adopted based on the analytical target cascading (ATC) method. In this model, the lower level dispatches each element in VMG from the standpoint of VMG's own interests, and an objective function of maximizing the VMG's benefits is constructed. The upper level dispatches each element in ADN from the perspective of ADN's economy and reliability, on this basis, a synthetic objective function is built. In addition, the ACT method is used to solve the coupling problem caused by the existence of interaction variables between the upper and lower levels, and ultimately to achieve win-win cooperation between ADN and VMG levels. Moreover, to reduce the computational complexity of the model and speed up the solving process, the second-order cone programming is employed in the proposed model to linearize the power flow calculation of the distribution network. Finally, simulation studies are conducted on the IEEE 18-bus distribution test systems to illustrate the feasibility of the proposed model. The stability and effectiveness of the model are verified by various comparisons.

INDEX TERMS Active distribution network, virtual micro-grid, bi-level model, analytical target cascading, second-order cone programming.

NOMENCLATURE

ABBREVIATIONS

ADN	Active distribution network
VMG	Virtual micro-grid
ESSs	Energy storage systems
RES	Renewable energy sources
CB	Capacitor banks
DG	Distribution generation
PV	Photovoltaic
ATC	Analytical target cascading
RL	Response load

SETS

G	Set of VMG in the lower model
$D_i/Q_i/E_i$	Set of DG/PV/ESS in the VMG_i
H	Set of scheduling time
N	Set of distribution network nodes
S/K	Set of DG/ESS in ADN
$u(j)$	The terminal node set of the branch with j as the first node in power grid
$v(j)$	Terminal node set of the branch with j as the first node in power grid

PARAMETERS

$C_{dis,t}$	Electricity purchase price of VMG at time t
$C_{rl,t}$	RL unit response cost at time t
$C_{PV,t}$	The unit output cost of PV at time t
R_e	Transaction price of unit carbon emissions

The associate editor coordinating the review of this manuscript and approving it for publication was M. Jahangir Hossain.

μ_k, η_k	Carbon emission intensity /Carbon credit under the unit output of generator
$C_{eo,k}, C_{ins,k}, L_k$	operation and maintenance Cost/Installation cost/Service life of ESS_k
$C_c(t)$, $C_d(t)$	The unit charge/discharge price of ESS_k at time t
η_{ch}, η_{dis}	ESS charging/discharging efficiency
$P_{ch,i}^{\max}, P_{dis,i}^{\max}$	Maximum charging/discharging power of ESS_i
$E_{soc,i}^{\max}$	Capacity limitation of ESS_i
$P_{DG_i}^{Dis,\max}, Q_{DG_i}^{Dis,\max}$	Maximum active and reactive power of DG_i
$N_{i,t}^{CB,\max}$	Maximum number of CB commissioning groups
B_{CB}^{lim}	Maximum number of CB actions in a cycle

VARIABLES

$E_{load,t}^{VMG_i}$	Cost of RL in VMG_i at time t
$E_{DGs,t}^{VMG_i}$	Cost of DGs in VMG_i at time t
$E_{ESSs,t}^{VMG_i}$	Cost of ESSs in VMG_i at time t
$E_{co_2}^{VMG_i}$	Revenue from carbon trading in VMG_i
$P_{sell,t}^{VMG_i}$	The power of VMG_i sales at time t
$u_{t,k}^{charge}, u_{t,k}^{discharge}$	Charging and discharging state of ESS_k
$E_{soc,i,t}$	Charging State of ESS_i at time t
$Q_{i,t}^{CB}$	Reactive Power Compensation of CB Connected on i Node at time t
$Q_{i,setp}^{CB}$	Reactive power compensation for each group of CB
$N_{i,t}^{CB}$	The number of CB operating groups at time t
$B_{i,t}^{CB}$	On-off state of CB at time t
$P_{ij,t}, Q_{ij,t}$	Active and reactive power flowing through branch j-i at time t
$P_{j,t}, Q_{j,t}$	Active and reactive power injected by node j at time t
$P_{j,DG,t}, Q_{j,DG,t}$	Active and reactive power of DG at time t connected with j-node
$Q_{j,CB,t}$	Reactive power of CB at time t connected with node j
$P_{j,t}^{VMG}, Q_{j,t}^{VMG}$	Active and reactive power of VMG at time t connected to node j
$P_{j,d,t}, Q_{j,d,t}$	Active and reactive load of node j at time t

I. INTRODUCTION

With the increasing penetration of distributed generation in distribution network, in order to realize the active management and scheduling of internal resources in distribution network, various countries have successively studied the active distribution network (ADN) technology under the framework of smart grid. The objective of the ADN is to control distributed generation (DG) equipments and load side resources to improve power supply reliability and power quality, as well as to reduce the loss of distribution network. Relevant researches show that active management of DG supply and optimal dispatching of all kinds of controllable loads in distribution network generation have become important measures to achieve the above objectives [1]–[3].

With the rapid development of smart grid, power market and intelligent load control technology, demand response technology aiming at the active interaction between distribution network and load has been widely concerned [4]–[6]. At the same time, the collaborative development of DGs and various controllable loads is not only helpful to accomplish the goal of ADN but also significant to satisfy customer's demand for diversified, personalized and interactive services [7]. Aiming at the coordinated dispatch problem among distribution network, load, and distributed generation, some related scholars have conducted in-deep research.

Lu *et al*. [8] propose a collaborative dispatching model between the distribution network and large-scale renewable energy, and use the balanced Q(λ)-learning method to obtain the optimal scheduling strategy of multi-stakeholder game coordination, so as to effectively improve the enthusiasm and fairness of new stakeholders participating in grid coordination and optimization in ADN. However, the balanced Q(λ)-learning method will cause "dimension disaster" when there are many variables, which leads to the failure of solving the model. In addition, solving the model is time-consuming because of its nonlinearity. Li *et al.* [9] propose a multi-objective, multi-level model for active distribution system expansion planning with high-penetration renewable energy sources (RESs) and energy storage systems (ESSs) considering the interests of different participants in the grid. The improved Prato-based particle swarm optimization (PSO) algorithm is utilized to solve the model. However, this method also has a problem that the solution time is long, which is not conducive to the real-time dispatch of the power grid. More than this, the final outcome obtained from this model is an optimal solution set with uncertainty. Guo *et al.* [10] develop a hybrid integer cone programming based voltage and reactive power collaborative optimization model for ADN to optimize the network. Although the model solves the problem that the solution time is considerably large due to the nonlinearity, it loses sight of different participants' interests. Moreover, in order to increase the consumption of renewable energy and reduce the uncertainty of the system, Zhu *et al.* [11] conduct a multi-stage active distribution network scheduling method with renewable energy, but the interests of distributed energy owners in active distribution networks are still not considered. Golshannavaz *et al.* [12] focus on a joint stochastic energy and reserve scheduling problem in the distribution system and propose a novel high-performance energy management system (EMS) making use of automatically controlled switches to optimize energy in the distribution network. Similarly, the role of costumers in energy management is neglected. Huang *et al.* [13] considers both the speed of solving the model and the interests of multiple participants and put forward a multivariate cooperative optimal dispatching model for optimizing the interests of all parties in active distribution network, but the model weakens the impact of electricity price in different periods. Mazidi *et al.* [14] concentrate on incorporating responsive in day-ahead scheduling planning of ADN. A new controllable mixed-integer linear programming (MILP) optimization technique is proposed to realize the pricing of electricity, which maximizes the benefits of the power grid and users. However, the reliability of ADN is not included in the process of price setting. The emerging of competitive players with different interests changes the previous regulation mode of the active distribution network, and different dispatching models are desired. DG operators and users are both accounted for in the optimization dispatch model in [15], [16], where a double layer dispatch model is proposed: The upper level optimizes the conflicting power between the distribution network and different stakeholders, while the lower level optimizes the objective of various stakeholders. Similarly, the reliability of distribution network is not considered too much in the optimization process.

By analyzing the above literatures, it can be find that in the process of constructing the optimal dispatching model of active distribution network, researchers share different emphases on the interests of different participants, the reliability of distribution network and the speed of solving the model. But in Chinačwith the deepening of the reform of the electric power system, strong power generation enterprises will be allowed to participate in the electricity market. Therefore, there will be a large number of distributed power supply in the distribution network, which will be invested and constructed by operators, and will supply power to using area independently. We call the regional power grid invested by operators or multi-stakeholders as virtual micro-grid (VMG), and the regional power grid is not uniformly scheduled by the distribution grid. These VMGs aim at maximizing their own profits, and have independent dispatching units, which are not entirely dependent under the unified dispatch of the distribution network [17]. Accordingly, the mode of weakening the stakeholders of different participants will no longer adapt to the current situation [11], [18]. At the same time, the power companies pay more attention to the quality of service, which makes the users' requirements for the reliability of distribution network further improved. The optimization model without considering the reliability of distribution network will no longer adapt to the current situation [19]. Additionally, due to the high proportion of renewable energy in the distribution network, the uncertain output of renewable energy will make the operation of the distribution network change dramatically in a short time. For this point, the iteration optimization method of power flow in distribution network based on bionic algorithm is difficult to meet the time requirement of model calculation due to the long solving time [8], [10], [34].

To figure out the problems mentioned above, a bi-level linearized dispatching model of active distribution network with the consideration of multi-stakeholder participation, the power supply reliability of ADN, and the solving speed of the model is developed in this paper, in which the VMG as the lower level of the model and ADN as the upper level. The main contributions are summarized as follows:

(1) We propose the concept of VMG, on this basis, a bi-level linearized dispatching model between ADN and VMG is constructed, which fully pays attention to multiple independent stakeholders. The model can achieve cooperative optimization between ADN and VMG according to the electricity price at different time from the perspective of multiple stakeholders.

(2) In the process of optimizing the upper level model, not only the goal of the economy but also the voltage of the distribution network is considered, which makes the optimization of the distribution network more integrated.

(3) The second-order cone optimization is utilized to linearize the power flow of the distribution network, and the dispatching problem of the distribution network is transformed into a convex optimization problem to accelerate the solving speed of the model.

(4) There are transmission variables coupled with other regions in the upper and lower models, which lead to the models cannot be solved independently. In view of this difficulty, the ATC method is utilized in this paper because of its capability in handling multi-level, multi-body coordination and optimization problems. The transmission variables between the upper and lower levels are introduced into the ATC method in the form of the penalty function to decouple the upper and lower levels model and obtain the solution of the optimal model.

The remainder of this paper is organized as follows. The framework of the proposed model is introduced in Section II. Section III describes the problem and formulates the model. Aiming at enhancing the speed of solving the model, the power flow calculation method based on second-order cone optimization and the ATC method is presented in Section IV. Section V analyzes the simulation results. Section VI concludes.

II. FRAMEWORK OF BI-LEVEL INTERACTIVE ENERGY SCHEDULING MODEL BETWEEN ADN AND VMG

A. VIRTUAL MICRO-GRID

Virtual micro-grid(VMG) mainly refers to the regional power grid that is not uniformly scheduled by the distribution grid, which can maximize revenue by coordinating and controlling internal resources. VMG mainly includes three types of grids. The first type is a user-built micro-energy grid with renewable energy, which can not only provide energy to users but also conduct electricity trading with the distribution network. Such a grid is typically operated with the objective of minimizing operating costs, without considering the safety/economy of the distribution grid. The second type of grid is formed according to the reform of China's power system. It is mainly a grid managed by a new power sale company, which is formed by the reform of the power system. During the operation of such grids, the company usually puts its economic benefits first and is not aware of the distribution grid's operation. The third type of grid is a generalized virtual power plant introduced by [20], which is composed of various types of distribution generations and loads. Such a grid has an independent scheduling system, yet it also fails to take into account the operation of the distribution grid.

B. MODEL FRAMEWORK

In the traditional operation process, VMG only focuses on its own economy, ignoring the operating state of the distribution grid. However, the security and economy are important factors in the dispatching process of the distribution network, which should be taken seriously. VMG and ADN are controlled and operated by operators and power gird dispatchers respectively. Therefore, the access of VMG brings great obstacles to the operation of the distribution grid. With the improvement of the automation level of distribution grid, supervisory control and data acquisition (SCADA) system has reached full coverage, which enables staff to obtain real-time operational information about the distribution grid and provides the possibility for the interconnection of VGM and ADN.

To better achieve coordination between VMG and ADN, a bi-level linearized interactive operation model is proposed. The decision category of the model is a problem with two decision making levels where each decision maker tries to optimize its own objective in an interactive process. The upper level is adopted to optimize the economic and reliability problem of ADN. The lower level serves to optimize the operation scheduling of VGM, including renewable energy source (RES), energy storage system (ESS), distribution generation (DG), and response load (RL), to maximize the economic benefits of VGM. The optimization results from the lower level are fed back to the upper level to calculate the economic and security of the distribution. Similarly, the results from the upper level will be fed back to the lower level to calculate the economic of the VMG. The framework of the bi-level model is shown in Figure 1.

III. PROBLEM FORMULATION

A. OPTIMIZATION OBJECTIVE

1) OBJECTIVE FUNCTION OF LOWER LEVEL

The lower level model focuses on maximizing VMG benefits by scheduling RES, ESS, DG, and RL. For large-scale renewable energy, this paper introduces the carbon trading mechanism to reduce the output cost of renewable energy, and further increase the benefits of VMG. In order to facilitate the analysis, photovoltaic (PV) will be used instead of RES. The objective function of the lower model is shown in Eq. (1), and the detailed expression of each item contained therein is

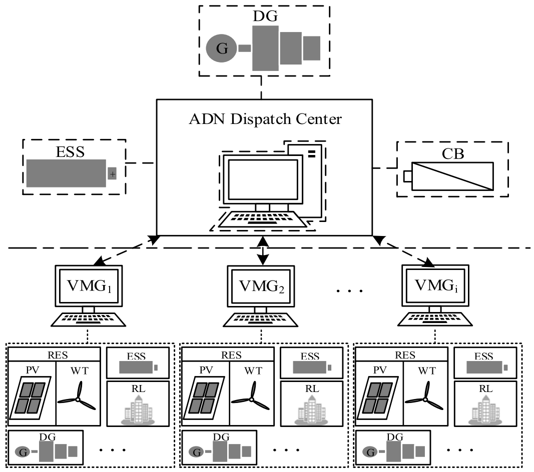

FIGURE 1. Framework of bi-level model between ADN and VMG.

as shown in Eqs. (2)-(7).

$$F_{low} = \max \sum_{VMG_i=1}^{G} \left\{ \sum_{t=1}^{H} \begin{bmatrix} C_{dis,t} P_{dis,t}^{VMG_i} + E_{PVs,t}^{VMG_i} \\ +E_{DGs,t}^{VMG_i} + E_{ESSs,t}^{VMG_i} \\ +E_{load,t}^{VMG_i} - C_{sell,t} P_{sell,t}^{VMG_i} \end{bmatrix} - E_{co_2}^{VMG_i} \right\} \tag{1}$$

$$E_{load,t}^{VMG_i} = C_{rl,t} P_{rl,t}^{VMG_i} \tag{2}$$

$$E_{DGs,t}^{VMG_i} = \sum_{k=1}^{D_i} \left[a_k^{VMG_i} P_{k,t}^{VMG_i} + c_k^{VMG_i} \right] \tag{3}$$

$$E_{PVs,t}^{VMG_i} = \sum_{k=1}^{Q_i} C_{PV,t} P_{k,t}^{VMG_i} \tag{4}$$

$$E_{co_2}^{VMG_i} = R_e \sum_{t=1}^{H} \left[\sum_{k=1}^{Q_i} \eta_k P_{PV,k,t} - \left(\sum_{i=1}^{D_i} \mu_k P_{k,t} - \sum_{i=1}^{D_i} \eta_k P_{k,t} \right) \right] \tag{5}$$

$$E_{ESSs,t}^{VMG_i} = \sum_{k=1}^{E_i} \left\{ \begin{array}{c} \left(C_{eo,k} P_{ESS,t,k}^{VMG_i} + \frac{C_{ins,k}}{365 \times 24 L_k} \right) \Delta t \\ + \left[\left(u_{t,k}^{ch\arg e} C_c(t) - u_{t,k}^{disch\arg e} C_d(t) \right) \right. \\ \left. \times P_{ESS,t,k}^{VMG_i} \right] \Delta t \end{array} \right\} \tag{6}$$

$$P_{sell,t}^{VMG_i} = P_{dis,t}^{VMG_i} - P_{load,t}^{VMG_i} + P_{PVs,t}^{VMG_i} + P_{ESSs}^{VMG_i} + P_{DGs,t}^{VMG_i} \tag{7}$$

where Eqs. (2)-(6) represent the RL cost, DG output cost, PV output cost, carbon dioxide emission cost, and ESS charge and discharge cost in VMG_i, respectively. Eq. (7) represents the selling power of VMG_i. If the result of $P_{sell,t}^{VMG_i}$ is less than zero, then let $P_{sell,t}^{VMG_i} = 0$.

2) OBJECTIVE FUNCTION OF UPPER LEVEL

The upper level serves as the planning of networks from the angle of ADN operation. Different from the traditional planning approach, ADN requires the best alternative with a multi-objective approach [21]. In this paper, two objectives are adopted, including economy and reliability.

a: ECONOMIC OBJECTIVE

The exchange power between the ADN and the VGM, the energy storage on the side of the ADN, the output of the distributed generator, and the exchange power with the upper transmission network constitute the economic objective function, as shown in Eq. (8), and the detailed expression of each item contained therein is as shown in Eqs. (9)-(13).

$$f_1 = \min \frac{1}{\sum_{t=1}^{H}\sum_{j=1}^{N} C_{tran,t}P_j^t} \times \sum_{t=1}^{H}\left[\begin{array}{l} C_{tran,t}P_{tran,t}+E_{co_2,t}^{Dis}+\sum_{i=1}^{G} C_{VMG,t}P_{F,t,i} \\ +E_{DGs,t}^{Dis}+E_{ESSs,t}^{Dis}+C_{tran,t}P_{loss,t} \end{array}\right] \tag{8}$$

$$P_{F,i,t} = P_{sell,t}^{VMG_i} \tag{9}$$

$$E_{DGs,t}^{Dis} = \sum_{i=1}^{S}\left[a_i^{Dis}P_{i,t}^{Dis}+b_i^{Dis}\right] \tag{10}$$

$$E_{co_2,t}^{Dis} = R_e\sum_{t=1}^{H}\left(\sum_{i=1}^{S}\mu_i P_{i,t}^{Dis}-\sum_{i=1}^{S}\eta_i P_{i,t}^{Dis}\right) \tag{11}$$

$$P_{loss,t} = \sum_{i=1}^{N}\sum_{j\in u(i)} r_{ij}\frac{\left(P_{ij,t}\right)^2+\left(Q_{ij,t}\right)^2}{\left(U_{i,t}\right)^2} \tag{12}$$

$$E_{ESSs,t}^{Dis} = \sum_{i=1}^{K}\left\{\begin{array}{c} \left(C_{eo,i}P_{ESS,t,i}^{Dis}+\frac{C_{ins,i}}{365\times 24L_i}\right)\Delta t \\ +\left[\left(u_{t,i}^{ch\arg e}C_c(t)-u_{t,i}^{disch\arg e}C_d(t)\right)\right. \\ \left. P_{ESS,t,i}^{Dis}\right]\Delta t \end{array}\right\} \tag{13}$$

where Eq. (9) is equal to Eq. (7); Eqs. (10), (11), and (13) are similar to Eqs. (3), (5), and (6); Eq. (12) indicates the power loss during the operation of ADN, respectively. This paper holds that reactive power compensation device is the intrinsic asset of ADN, so the cost of reactive power compensation is not considered.

b: RELIABILITY OBJECTIVE

The most basic requirement for safe and stable operation of ADN is that the voltage is stable within the specified range. The average voltage deviation has become a key indicator for evaluating the reliability of ADN. The smaller the average voltage deviation, the higher the reliability. We aim to minimize the average voltage deviation and set it as the second objective, defined as Eq. (14).

$$f_2 = \min \frac{1}{H}\sum_{t=1}^{H}\sqrt{\sum_{i=1}^{N}\left(1-U_{i,t}\right)^2} \tag{14}$$

Reactive power compensation in ADN is close to voltage. Therefore, the realization of this objective requires the control of reactive power compensation devices in ADN and VMG.

c: CONVERSION MULTI-OBJECTIVE FUNCTION

Considering the economic and reliability factors of ADN, the comprehensive objective function F_{up} is constructed, as shown in Eq. (15). According to the multi-objective comprehensive evaluation method proposed in [22], the optimal weight of each sub-subjective in the multi-objective function can be determined. The weight constraint is $\alpha + \beta = 1$.

$$F_{up} = \min\left(\alpha f_1 + \beta f_2\right) \tag{15}$$

Eqs. (1)-(14) contains many constraints, which will be described and explained in detail in the following.

B. OPTIMIZATION OBJECTIVE

1) CONSTRAINTS OF LOWER LEVEL

a: RL CONSTRAINTS

Continued in Eq. (2), in order to ensure that the RL in VMG can participate in the scheduling normally, RL should be limited to a certain range for hour t, as shown in Eq. (16). In addition, following Sattarpour *et al.* [23], RL is supposed to have a constant power factor (θ_{rl}), as shown in Eq. (17).

$$0 \le P_{rl,t}^{VMG_i} \le P_{rl,t}^{VMG_i,\max} \tag{16}$$

$$Q_{rl,t}^{VMG_i} = \tan\left[\cos^{-1}\left(\theta_{rl}\right)\right]\times P_{rl,t}^{VMG_i} \tag{17}$$

b: PV AND DG CONSTRAINTS

To alleviate the harmful effects of bi-directional power flow, PV output should be lower than its predicted value, as shown in Eq. (18). In this study, PV is supposed to have a constant power factor (θ_{PV}), as shown in Eq. (19)

$$0 \le P_{PVs,t}^{VMG_i} \le P_{PVs,t}^{\max} \tag{18}$$

$$Q_{PVs,t}^{VMG_i} = \tan\left[\cos^{-1}\left(\theta_{PV}\right)\right]\times P_{PVs,t}^{VMG_i} \tag{19}$$

For DG, since the power response speed of the micro gas turbine is faster, the climb constraint is not considered, and only the output is constrained. The constraints of active power output and reactive power output are shown in Eqs. (20) and (21), respectively.

$$0 \le P_{DG_i,t}^{VMG_i} \le P_{DG_i}^{VMG_i,\max} \tag{20}$$

$$0 \le Q_{DG_i,t}^{VMG_i} \le Q_{DG_i}^{VMG_i,\max} \tag{21}$$

c: ESS CONSTRAINTS

The operation of ESS should be strictly under the constraints of the periodic behaviors, the permissible ranges of state of charge (SOC) and charging/discharging power, as shown in Eqs. (22)-(26).

$$0 \le u_{t,i}^{ch\arg e}P_{ESS,t,i}^{VMG_i} \le P_{ch,i}^{\max} \tag{22}$$

$$0 \le u_{t,i}^{disch\arg e}P_{ESS,t,i}^{VMG_i} \le P_{dis,i}^{\max} \tag{23}$$

$$u_{t,i}^{ch\arg e}+u_{t,i}^{disch\arg e} \le 1 \tag{24}$$

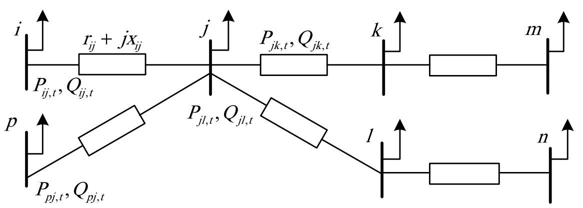

FIGURE 2. Active distribution network with radial operation.

$$E_{soc,t,i}+u_{t,i}^{ch\arg e}P_{ESS,t,i}^{VMG_i}\eta_{ch}\Delta t -\left(\frac{u_{t,i}^{disch\arg e}P_{ESS,t,i}^{VMG_i}}{\eta_{dis}}\right)\Delta t=E_{soc,t+1,i} \quad (25)$$

$$E_{soc,i}^{\max}\times 20\% \le E_{soc,i,t}\le E_{soc,i}^{\max}\times 90\% \quad (26)$$

2) CONSTRAINTS OF UPPER LEVEL

In the upper level, it mainly involves ESS, DG, and power flow constraints of ADN operation. Since the voltage deviation is involved in the objective function, the reactive compensation needs to be taken into account in the upper optimization model. According to the actual situation, this paper will use the capacitor banks (CB) to perform reactive power compensation for ADN. The ESS and DG constraints are similar to those in the lower model, and the CB and power flow constraints are described in detail below.

a: CB CONSTRAINTS

Due to the restriction of manufacturing technology and service life of the equipment, the number of CB operation in the scheduling cycle is limited, and each switching of the CB is operated in groups, so the CB operation should meet the following constraints.

$$\begin{cases} Q_{i,t}^{CB}=N_{i,t}^{CB}Q_{i,step}^{CB} \\ N_{i,t}^{CB}\le N_i^{CB,\max},\ N_{i,t}^{CB}\in int \\ B_{i,t}^{CB}\in\{0,1\} \\ \sum_{t=1}^{T-1}B_{i,t}^{CB}=B_{CB}^{lim} \\ B_{i,t}^{CB}Q_{i,step}^{CB}\le\left|Q_{i,t+1}^{CB}-Q_{i,t}^{CB}\right|\le B_{i,t}^{CB}N_i^{CB,\max}Q_{i,step}^{CB} \end{cases} \quad (27)$$

b: POWER FLOW CONSTRAINT

Figure 2 shows the ADN with radial operation in the upper optimization model, the corresponding power flow constraints are as follows [24]:

For node j, there are the following equality constraints for active power and reactive power.

$$\sum_{i\in u(j)}\left[P_{ij,t}-r_{ij}\frac{P_{ij,t}^2+Q_{ij,t}^2}{U_{i,t}^2}\right]=\sum_{k\in v(j)}P_{jk,t}+P_{j,t} \quad (28)$$

$$\sum_{i\in u(j)}\left[Q_{ij,t}-r_{ij}\frac{P_{ij,t}^2+Q_{ij,t}^2}{U_{i,t}^2}\right]=\sum_{k\in v(j)}Q_{jk,t}+Q_{j,t} \quad (29)$$

$$P_{j,t}=P_{j,DG,t}-u_{t,j}^{ch\arg e}P_{j,ESS,t}^{Dis}+u_{t,j}^{disch\arg e}P_{j,ESS,t}^{Dis}-P_{j,d,t}+P_{j,t}^{VMG} \quad (30)$$

$$Q_{j,t}=Q_{j,DG,t}+Q_{j,CB,t}+Q_{j,t}^{VMG}-Q_{j,d,t} \quad (31)$$

For the branch ij, there is the following equality constraint:

$$U_{j,t}^2=U_{i,t}^2-2\left(r_{ij}P_{ij,t}+x_{ij}Q_{ij,t}\right)+\left(r_{ij}^2+x_{ij}^2\right)\frac{P_{ij,t}^2+Q_{ij,t}^2}{U_{i,t}^2} \quad (32)$$

c: OTHER CONSTRAINTS

The following constraint determines the proper voltage profile for all nodes in ADN. For substation bus, the voltage magnitude remains constant and equal to 1.

$$\begin{cases} U_{\min}\le U_{i,t}\le U_{\max} \\ U_{1,t}=1 \end{cases} \quad (33)$$

Moreover, the following constraints ensure that each node does not exceed its allowable power range and that each line does not exceed its maximum power transmission range.

$$\sqrt{P_{j,t}^2+Q_{j,t}^2}\le S_j^{\max} \quad (34)$$

$$\sqrt{P_{ij,t}^2+Q_{ij,t}^2}\le S_{ij}^{\max} \quad (35)$$

IV. SOLVING APPROACH

A. LINEARIZATION OF POWER FLOW USING SECOND-ORDER CONE PROGRAMMING

In the upper optimization model, decision variables include ESS charging and discharging power, CB operating power, and DG output at each moment, etc., accordingly, it is an ADN dynamic optimization model with continuous and discrete variables. In addition, the power flow constraints presented by Eqs. (28), (29) and (32) in the model are quadratic equations, leading to a mixed-integer non-convex non-linear problem, which belongs to NP problem [27]. Using the non-linear solution method will make the solving speed of the model longer. Therefore, the linearization of power flow calculation is the first task we need to do. Current linearized power flow is usually carried out by second-order cone programming [25].

The standard form of second-order cone programming (SOCP) is as follows [26]:

$$\min_{x_i}\left\{\mathbf{c}^T\mathbf{x}|\mathbf{A}\mathbf{x}=\mathbf{b},x_i\in K,i=1,2,\ldots,N\right\} \quad (36)$$

where $\mathbf{x}\in\mathbf{R}_N$, $\mathbf{b}\in\mathbf{R}_M$, $\mathbf{c}\in\mathbf{R}_N$, $\mathbf{A}_{M\times N}\in\mathbf{R}_{M\times N}$, K is shown as follows:

$$K=\left\{x_i\in\mathbf{R}_N|y^2\ge\sum_{i=1}^{N}x_i^2,y\ge 0\right\} \quad (37)$$

Based on the characteristics of SOCP, the power flow equation can be relaxed. Let $\tilde{I}_{ij,t}=(P_{ij,t}^2+Q_{ij,t}^2)/U_{i,t}^2$ and $\tilde{U}_{i,t}=U_{i,t}^2$, the original Eqs. (28), (29) and (32) can be transformed into Eqs. (38)-(40).

$$\sum_{i\in u(j)}\left(P_{ij,t}-\tilde{I}_{ij,t}r_{ij}\right)=\sum_{k\in v(j)}P_{jk,t}+P_{j,t} \quad (38)$$

$$\sum_{i\in u(j)}\left(Q_{ij,t}-\tilde{I}_{ij,t}r_{ij}\right)=\sum_{k\in v(j)}Q_{jk,t}+Q_{j,t} \tag{39}$$

$$\begin{aligned}\tilde{U}_{j,t}&=\tilde{U}_{i,t}-2\left(r_{ij}P_{ij,t}+x_{ij}Q_{ij,t}\right)\\&\quad+\left(r_{ij}^2+x_{ij}^2\right)\tilde{I}_{ij,t}\end{aligned} \tag{40}$$

Then, following Liu *et al.* [27], let $\tilde{I}_{ij,t}\geq(P_{ij,t}^2+Q_{ij,t}^2)/\tilde{U}_{i,t}$, this inequality constraint is further transformed into the standard second-order cone by equivalent deformation, as shown in Eq. (41).

$$\left\|\begin{matrix}2P_{ij,t}\\2Q_{ij,t}\\\tilde{I}_{ij,t}-\tilde{U}_{i,t}\end{matrix}\right\|_2\leq\tilde{I}_{ij,t}+\tilde{U}_{i,t} \tag{41}$$

Then, Eqs. (28), (29), and (32) can be replaced by Eqs. (38)-(41), and flow constraints are successfully transformed from nonlinear to linear.

B. A HIERARCHICAL TWO-LEVEL OPTIMIZATION METHOD

If the ADN and VMGs are independent of each other and there is no connection between them, we can use the security-constrained unit commitment (SCUC) algorithm to solve the upper and lower models to obtain the optimal scheduling strategy [28], [29]. However, the ADN and VMGs are linked together in this paper, and the optimal operating point of one will affect the operating point of the other. In order to solve this problem and find the optimal operating point of the ADN and VMGs, a hierarchical two-level optimization method named analytical target cascading (ATC) is considered.

ATC method is mainly used to solve multi-level and multi-body coordination and optimization problems. It allows each optimization subject in the hierarchy to make independent decisions while at the same time obtaining the overall optimal solution of the problem through coordination and optimization. As ATC has the advantages of unlimited series, easy parameter selection, and different optimization forms for sub-problems of the same level, it also overcomes the phenomenon that the traditional dual decomposition algorithm based on Lagrange relaxation is prone to repeated oscillation in the iteration. Therefore, it is usually utilized to address large-scale system optimization problems [30], [31]. The convergence of ATC for solving convex optimization problems has been strictly proved in Michelena *et al.* [32].

Since the ADN and VMGs are actually connected together, there are transmission variables coupled with other regions in both optimization modules, leading to the model cannot be solved independently. In this paper, the penalty function of the transmission variable is added to the ATC to achieve complete decoupling of inter-region optimization. Specific modeling principle are described in appendix A.

After introducing the penalty function, the upper and lower optimization objective functions are reconstructed.

The objective function of the upper model with respect to ADN is modified to:

$$\begin{aligned}F_{up\_finally}&=F_{up}+\sum_{t=1}^{H}\sum_{i=1}^{G}\\&\times\left\{\begin{aligned}&\left[v_{i,p,t}\ \ v_{i,q,t}\right]\begin{bmatrix}P_{up,t,i}-\overline{P_{low,t,i}}\\Q_{up,t,i}-\overline{Q_{low,t,i}}\end{bmatrix}\\&+\left[\left[w_{i,p,t}\ \ w_{i,q,t}\right]\begin{bmatrix}P_{up,t,i}-\overline{P_{low,t,i}}\\Q_{up,t,i}-\overline{Q_{low,t,i}}\end{bmatrix}\right]^2\end{aligned}\right\}\end{aligned} \tag{42}$$

The objective function of the lower model with respect to VMG_i is modified to:

$$\begin{aligned}F_{low\_finally}&=F_{low}+\sum_{t=1}^{H}\sum_{i=1}^{G}\\&\times\left\{\begin{aligned}&\left[v_{i,p,t}\ v_{i,q,t}\right]\begin{bmatrix}\overline{P_{up,t,i}}-P_{low,t,i}\\\overline{Q_{up,t,i}}-Q_{low,t,i}\end{bmatrix}\\&+\left[\left[w_{i,p,t}\ w_{i,q,t}\right]\begin{bmatrix}\overline{P_{up,t,i}}-P_{low,t,i}\\\overline{Q_{up,t,i}}-Q_{low,t,i}\end{bmatrix}\right]^2\end{aligned}\right\}\end{aligned} \tag{43}$$

where $v_{i,p,t}$, $v_{i,q,t}$, $w_{i,p,t}$, and $w_{i,q,t}$ are algorithm multipliers, $P_{up,t,i}$ and $Q_{up,t,i}$ are the active and reactive power of VMG_i after upper optimization at time t, and these two values will be transmitted to the ADN level for optimization. $P_{low,t,i}$ and $Q_{low,t,i}$ are the active and reactive power of ADN after lower optimization at time t, and these two values will be transmitted to the VMG level for optimization. $\overline{P_{up,t,i}}$, $\overline{Q_{up,t,i}}$, $\overline{P_{low,t,i}}$, and $\overline{Q_{low,t,i}}$ are values of coupling variables obtained from adjacent regions, which are known variables. By setting the penalty function, the coupling variables can be as close as possible to the boundary power values transmitted by adjacent regions during the calculation process, and eventually reach consistency.

C. SOLVING FLOW

There are two different optimization procedures to deal with these two levels, respectively. The optimization procedure of upper and lower level transfer boundary variables to each other, as shown in Figure 3.

The first step is to optimize the lower level scheduling. Firstly, the algorithm multipliers and the virtual injection power of VMG ($\overline{P_{up,i,t}}$, $\overline{Q_{up,i,t}}$) are initialized. In addition, let the number of iterations be $k=1$ and get the transaction price of VMG and ADN. Then, the boundary exchange power $P_{low,i,t}^k$ and $Q_{low,i,t}^k$ of the lower model can be calculated according to Eq. (43), Eqs. (2)-(7), and Eqs. (16)-(26), and then transferred to the upper model. The second step is to optimize the upper level scheduling. Firstly, the transaction price of transmission network and ADN, and the transaction price of VMG and ADN are obtained. Then, considering the security constraints of ADN, the power flow is linearized by second-order cone programming. By using Eqs. (9)-(13),

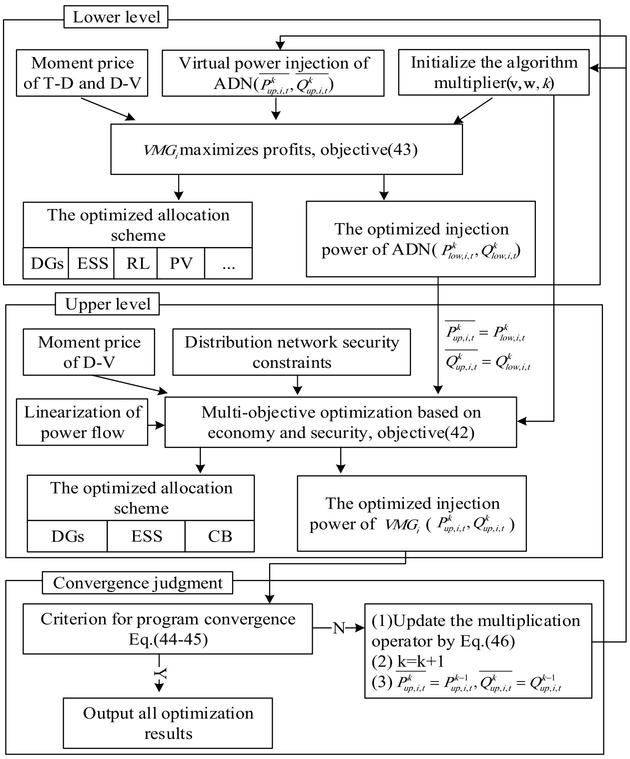

FIGURE 3. Bi-level optimization flow chart based on ATC.

Eqs. (20)-(27), and Eqs. (38)-(42), the AND optimal scheduling sub-problem can be solved, from which a set of optimal VMG switching power is obtained. After that, Eqs. (44)-(45) are applied to determine whether the loop converges or not, and if so, data of each device in the upper and lower levels is output, and the iteration terminates; Otherwise, the exchange power data is transferred to the lower level, the algorithm multipliers are updated according to Eq. (46), and the iteration continues.

$$\left|\begin{matrix} P^k_{up,t,i} - P^{k-1}_{low,t,i} \\ Q^k_{up,t,i} - Q^{k-1}_{low,t,i} \end{matrix}\right| \leq \left|\begin{matrix} \varepsilon_{1P} \\ \varepsilon_{1Q} \end{matrix}\right| \tag{44}$$

$$\left|\frac{F^k_{up\_finally} - F^{k-1}_{up\_finally}}{F^k_{up\_finally}}\right| \leq \varepsilon_2 \tag{45}$$

$$\begin{cases} \begin{bmatrix} v^{k+1}_{i,p,t} \\ v^{k+1}_{i,q,t} \end{bmatrix} = \begin{bmatrix} v^{k}_{i,p,t} \\ v^{k}_{i,q,t} \end{bmatrix} + 2\begin{bmatrix} w^{k}_{i,p,t} \\ w^{k}_{i,q,t} \end{bmatrix}^2 \begin{bmatrix} P_{up,t,i} - \overline{P_{low,t,i}} \\ Q_{up,t,i} - \overline{Q_{low,t,i}} \end{bmatrix} \\ \begin{bmatrix} w^{k+1}_{i,p,t} \\ w^{k+1}_{i,q,t} \end{bmatrix} = \begin{bmatrix} \gamma_p \\ \gamma_q \end{bmatrix} \begin{bmatrix} w^{k}_{i,p,t} \\ w^{k}_{i,q,t} \end{bmatrix} \end{cases} \tag{46}$$

where γ_p and γ_q are constants, Initial values of $v^k_{i,p,t}$, $v^k_{i,q,t}$, $w^k_{i,p,t}$ and $w^k_{i,q,t}$ generally take smaller constants.

V. CASE STUDY

A. INTRODUCTION OF CASE

In this section, IEEE18 distribution network is used as the text system, and the network topology is shown in Figure 4.

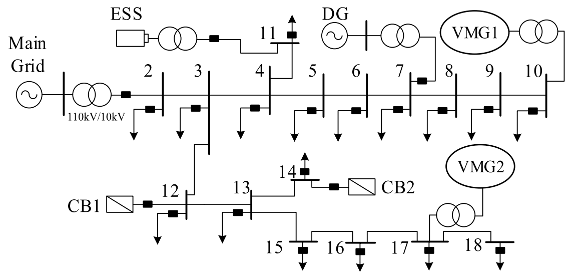

FIGURE 4. IEEE18-bus distribution test system.

TABLE 1. Time-of-use price for purchasing and selling electricity from AND to VMG.

Time interval	Specific time	Price/ ¥/kwh	
		purchasing electricity	Selling electricity
Peak time	10:00-12:00,18:00-20:00	0.834	0.784
Flat time	8:00-9:00，13：00-17:00,21:00-22:00	0.648	0.594
Valley time	0：00-7:00,23:00-24:00	0.17	0.13

Bus 12 and bus14 are connected with reactive compensation capacitors, bus 7 is connected with the active power of 1 MW, bus 10 and bus 17 are connected to VMG. VMGs contain DG, ESS, PV, and RL. The branch parameter, typical daily load parameter, typical PV output parameter, DG parameter, CBs parameter, and ESS parameter in ADN are shown in Appendix B. Table 1 presents the time-of-use price for purchasing and selling electricity from ADN to VMG.

The simulation of the case is carried out under the compiling environment of MATLAB 2016a. The model is built by the Yalmip optimization toolbox and solved by calling Cplex [33]. The computer used for simulation is configured as Intel(R)Core(TM)i5-5500 2.40GHz.

B. CASE ANALYSIS

Firstly, the power flow of the distribution network is linearized. Then, for the convenience of comparison, we consider three optimization models, including the VMG independent optimization, ADN independent optimization, and VMG&ADN joint optimization are simulated. VMG independent optimization means focusing only on the optimization of the upper level, and the obtained optimal outcome is transmitted to the ADN level for solution. With respect to ADN independent optimization, only the upper level is optimized according to the upper and lower load limits of VMG of each time, and the optimized result is transmitted to VMG for solution. When ADN&VMG joint optimization is simulated, ATC method is used to optimize the scheduling of upper and lower models to obtain the final optimization results. The parameters of ATC method are set as follows. The initial multipliers value of ATC method: $v_{i,p,t} = v_{i,q,t} = w_{i,p,t} = w_{i,q,t} = 0.5$, $\gamma_p = \gamma_q = 1.5$. The virtual injection power of VMG:$P^1_{up,i,t} = Q^1_{up,i,t} = 0$, $\varepsilon_{1P} = \varepsilon_{1Q} = \varepsilon_2 = 0.01$. The weights of the objective function in the ADN

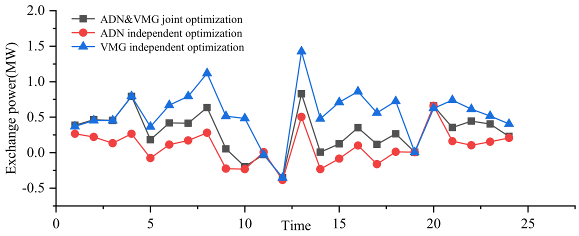

FIGURE 5. The load of VMG_1 under three optimization modes.

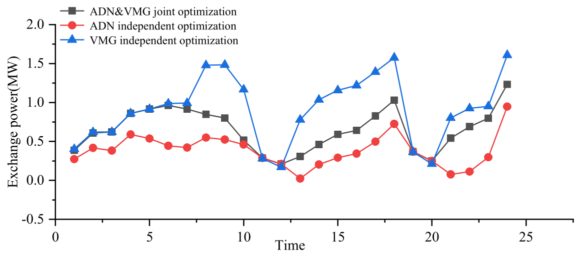

FIGURE 6. The load of VMG_2 under three optimization modes.

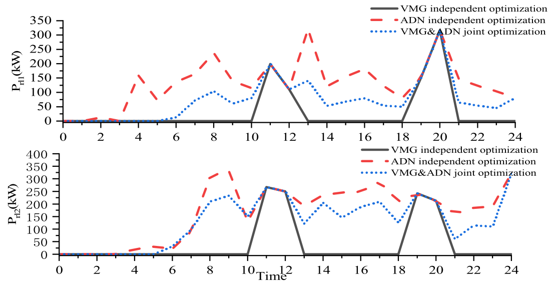

FIGURE 7. RL response in VMG_1 and VMG_2 under three optimization modes.

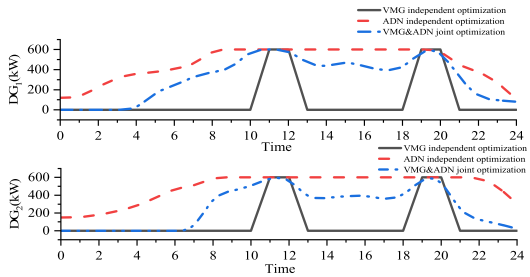

FIGURE 8. DG output in VMG_1 and VMG_2 under three optimization modes.

optimization level: $\alpha = 0.6$ and $\beta = 0.4$. Optimization results are shown in Figures 5-9.

Figures 5-6 depict the load conditions of VMG_1 and VMG_2 under three optimization modes, from which we can see that when VMG is optimized independently, VMG will mobilize the output of internal resources during the peak period of electricity price (10:00-12:00 & 18:00-20:00), so as to minimize the electricity purchased, and may even sell electricity to ADN. However, during the valley period of electricity price (0:00-7:00 & 23:00-24:00), VMG will purchase a large amount of power from ADN due to the high cost of VMG internal resources. During the flat period of electricity price, VMG will strictly control the output of its internal resources because the internal resource output cost is slightly higher than the purchase price. Overall, it can be seen from the scheduling results of VMG that the load of VMG is highly correlated with the time-of-use price with respect to its independent optimization. For the mode of ADN independent optimization, during the peak period, VMG needs to be dispatched to reduce the load demand due to the large load of ADN, to realize the economy and reliability of ADN operation. In the flat and valley period, the internal resources of VMG will be frequently mobilized by ADN. From the dispatching results of ADN independent optimization, it can be seen that to give priority to ADN's own interest, the load of VMG will be kept at a low level for a long time, resulting in a great loss to the economy of VMG. Importantly, the VMG & ADN joint optimization mode combines the advantages of the first two optimization modes, which not only improves the load of VMG and ensures the maximization of VMG's benefits during the valley period of electricity price, but also mobilizes part of internal resources of VMG in the flat price period, thereby reducing the load of VMG and improving the economic and reliability of ADN.

Figures 7 and 8 show the RL response and DG output in VMG_1 and VMG_2 under three optimization modes. It can be seen from the simulation results that the RL response cost and the DG output cost are higher than the purchase price of the flat and the valley period for VMG independent optimization, consequently, the RL and DG will participate in the grid interaction strictly according to the time-of-use price. When ADN is independently optimized, ADN will fully schedule the RL and DG output in the VMG, resulting in poor economics of the VMG. When VMG & ADN joint optimization, the RL and DG in the VMG will reduce the output during the valley period, and will participate in the ADN scheduling during the flat period. This joint optimization scheduling model takes into account the interests of both ADN and VMG, thus realizing the win-win situation. In addition, the introduction of carbon trading mechanism further reduces the cost of PV output, so PV in VMG does not reduce the output operation during the scheduling cycle.

Figure 9 shows the ESS dispatching results under three optimization modes, from which it can be known that when VMG independent optimization, the ESS in VMG will be charged during the valley period and discharged during the peak period to obtain the best interest of ESS. ADN independent optimization model ignores the economy of VMG, the ESS will be charged and dispatched during the flat period of electricity price, and moreover, the discharge capacity of ESS will be reduced during the peak period. As a result, the economy of ESS in VMG will be reduced. However, the ESS dispatching in the model of ADN and VMG joint optimization is a comprehensive process, which will decrease the charge of ESS in the flat period and increase the discharge of ESS in the peak period.

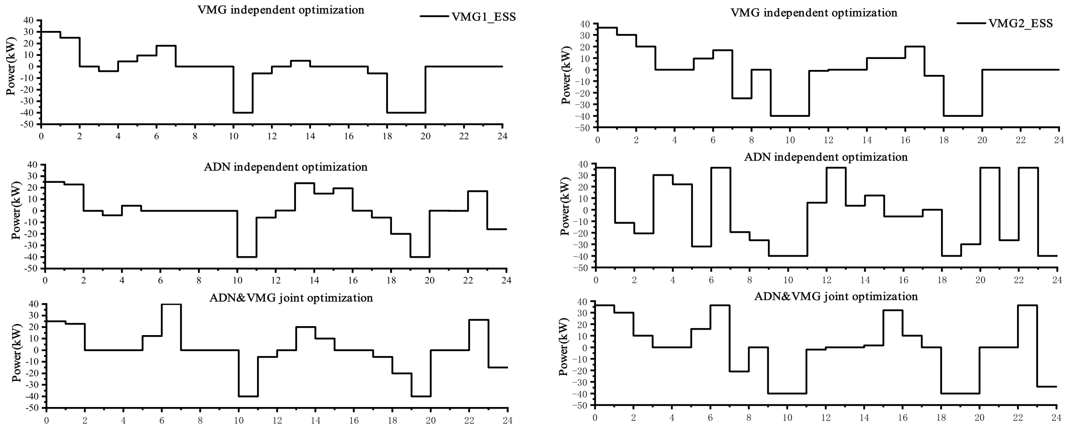

FIGURE 9. ESS charging and discharging status in VMG1 and VMG2 under three optimization modes.

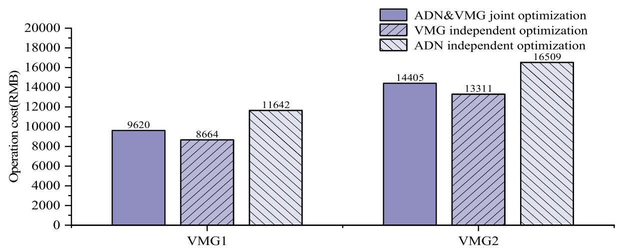

FIGURE 10. Operating costs for VMG under three optimization modes.

On this basis, the operating costs of VMG under three optimization modes can be obtained. As shown in Figure10, the operating cost of VMG reaches ceil with ADN independent optimization and touches floor with VMG independent optimization, respectively. ADN & VMG joint optimization can be treated as a compromise.

The simulation results of the ADN level are shown as follows. As can be seen from Figure 11, the voltage fluctuation of ADN is the greatest (0.8629) in the case that VMG is optimized independently, and the voltage situation obtained by ADN&VMG joint optimization is closer to the result obtained from ADN independent optimization. Figures 12-14 show the results of internal elements (CBs, ESS, DG) for ADN under three optimization models. From these three graphs, we can find that for the model of ADN independent optimization, the equipment in ADN will retain a certain margin because the VMG's internal resources are fully mobilized during the VMG operation process. The VMG independent optimizations will result in a decrease in equipment operating margin in ADN, while joint optimization operation is a reasonable trade-off between VMG and ADN.

On this basis, the results of the ADN level's optimization objectives under three optimization modes are shown in Figure 15. We can see that when the ADN runs based on the results of VMG independent optimization, the loss of the ADN is large (7.977 MW), the average voltage of the system is lower, and the reliability and economic operation indicators at the ADN level are poor, which are contrary to the results obtained based on AND independent optimization. Fortunately, the corresponding results with respect to economy and reliability under ADN&VMG joint optimization mode are more in common with the AND independent optimization mode.

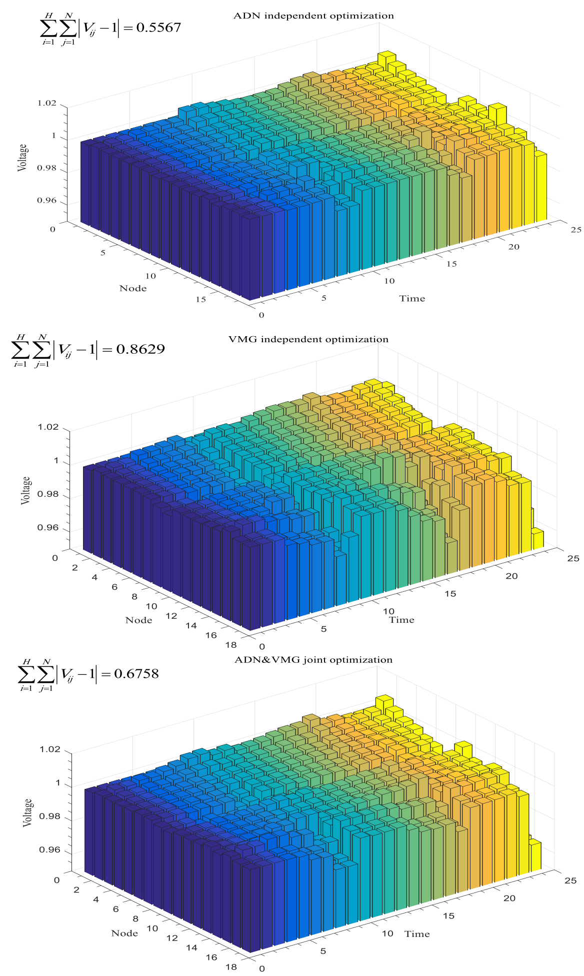

FIGURE 11. Voltage situation of ADN under three optimization modes.

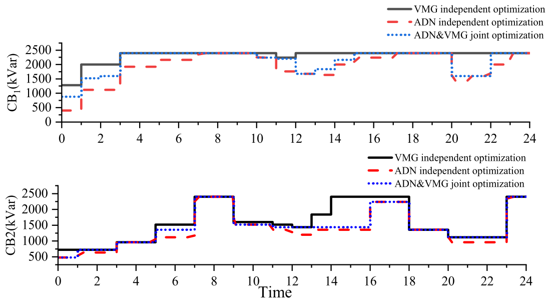

FIGURE 12. The state of CBs in ADN under three optimization modes.

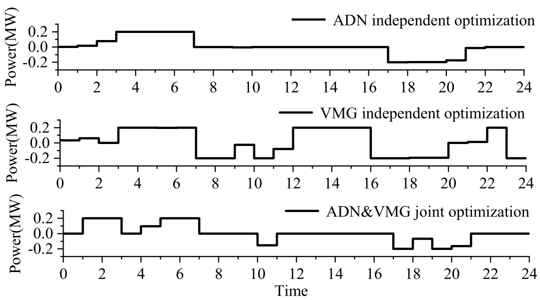

FIGURE 13. The state of ESS in ADN under three optimization model.

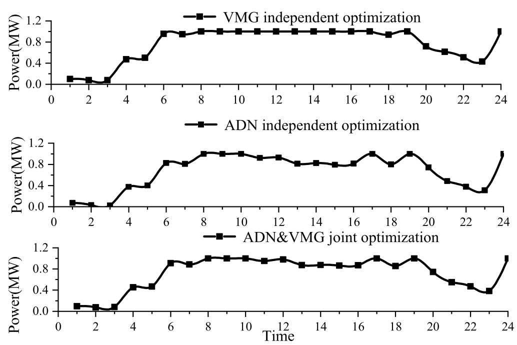

FIGURE 14. The state of DG in ADN under three optimization model.

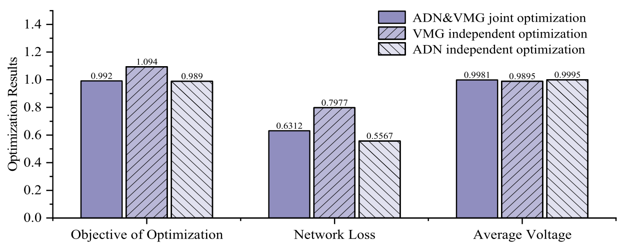

FIGURE 15. Results of ADN optimization objectives under three optimization modes. Note: to facilitate the presentation of the figure, the network loss value of ADN shown in the histogram is one tenth of the true value, for example, 0.6312=6.312/10, where 6.312 is the true network loss value.

The simulation results of the whole dispatching cycle show that the ADN independent optimization mode features the advantage of economy and reliability of ADN, but the operating cost is high due to VMG's interest is neglected. Additionally, although the operating cost of the VMG independent optimization mode is the lowest, it will result in increased network loss and a decline in voltage quality of ADN. ADN & VMG joint optimization mode can not only get the advantages of the first two modes but also overcome the shortcomings of both to a certain extent.

TABLE 2. Three optimization results at 9:00.

Parameter		VMG	VMG&ADN	ADN
VMG_1	P_{MT} / kW	0	400	600
	Q_{MT} / kVar	0	320	320
	ESS / kW	0	0.246	0.0306
	RL / kW	0	60.9	139.3
	PV / kW	182	182	182
	Exchange power / kW	514.36	53.48	-224.9
	Cost / yuan	413.36	428.26	446.05
VMG_2	P_{MT} / kW	0	450	600
	Q_{MT} / kVar	0	320	320
	ESS / kW	0	-5	-5
	RL / kW	0	232.9	332.9
	PV / kW	182	182	182
	Exchange power / kW	1482.4	794.49	544.49
	Cost / yuan	1040.6	1061.2	1074.3
ADN	P_{MT} / kW	1000	1000	950
	Q_{MT} / kW	320	320	320
	CB_1 / kVar	2400	2400	2400
	CB_2 / kVar	2400	2400	2400
	ESS / kW	-200	0	0

C. TYPICAL MOMENT ANALYSIS

In this section, a typical moment is analyzed. It can be seen from Table 2 that at 9:00, since the DG output cost and RL response cost are higher than the purchase price, neither of them will contribute when VMG independent optimization. At this point, VMG will absorb power from ADN, resulting in the lowest cost of VMG. When ADN independent optimization, the internal resources of VMG will be dispatched according to the situation of ADN to ensure that the ADN is in the optimal operation, but such results are accompanied by the highest cost of VMG at this moment. The joint optimization proposed in this paper has dual contributions, which not only improves the output of internal elements in VMG appropriately but also reduces the operation cost of VMG to a certain degree.

In addition, it is obvious in Figure 11 that the voltage of ADN is low at 9:00. According to table 2, the reactive power compensation devices of ADN under three optimization modes are in full compensation state. Joint optimization and ADN independent optimization can improve the reliability of the ADN by dispatching active and reactive power in VMG. On this basis, the optimizing objectives of ADN under three optimization modes can be obtained (see Table 3).

TABLE 3. Comparison and analysis of ADN optimizing objectives under three optimization modes at 9:00.

Parameter	VMG	VMG&ADN	ADN
Loss/MW	0.401	0.374	0.385
Average voltage	0.9822	0.9893	0.9950

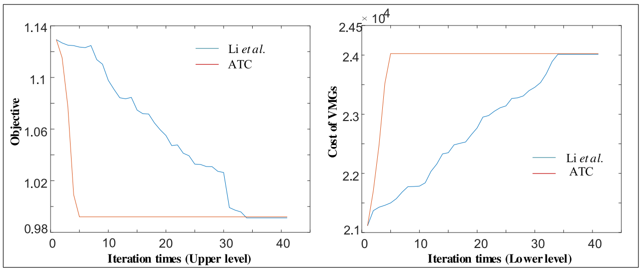

FIGURE 16. Iteration of two algorithms for the upper and lower objective functions.

TABLE 4. Comparison of the results of three method.

	Objective	Loss /MW	Voltage/p.u	Time /s	Iterations	Cost of VMGs/yuan
Li *et al.*	0.991	0.640	0.999	903.1	34	24013
Centralized	0.993	0.652	0.998	3	-	23997
ATC	0.992	0.631	0.998	9.4	5	24025

D. CORRECTNESS COMPARISON OF METHOD

In order to verify the effectiveness of the method, the method proposed in Li *et al.* [34] and the centralized optimization method are adopted to solve the case. According to Li *et al*, the upper level utilizes the multi-objective particle swarm optimization (PSO) method to optimize the model. In the optimization process, the calculation of power flow in the distribution network is realized by calling the Matpower program, which is not linearized. The lower model is optimized by the chaos PSO algorithm. The number of iterations is set to 40, and the convergence condition is $\varepsilon_{1P} = \varepsilon_{1Q} = \varepsilon_2 = 0.01$.

For the centralized optimization method, the objective functions of upper and lower models are added to the final objective function, and the model is solved by combining the upper and lower model constraints. The final results are shown in Table 4. The iteration of algorithms is shown in Figure16.

By comprising, we can find that although the optimization results of the proposed method are accordance with results obtained based on the above algorithm, the solution time in Li *et al* is longer since the power flow calculation is not linearized. Although the centralized optimization method has a faster solution speed, it has a premise, i.e., it requires to fully derive the VMG internal resource information, which does not meet the current situation. However, the method proposed in this paper can realize the rapid solution of the model on the basis of fully considering and respecting the interests of all parties.

TABLE 5. Solution results of the proposed model based on different algorithm packages.

Algorithmic Package	Time /s	Iterations	Objective	Loss /MV	Voltage/p.u	Cost of VMGs/yuan
Cplex	9.4	5	0.992	0.631	0.998	24025
Mosek	11.5	6	0.992	0.631	0.998	24025
Gurobi	9.7	5	0.992	0.631	0.998	24025

E. STABILITY COMPARISON OF THE METHOD

From the results of Table 5, we can see that the solution results of the proposed model based on various algorithm packages are highly consistent, which verifies the stability of the method.

VI. CONCLUSION

This paper attempts to solve the dispatching problem caused by the emergence of a new environment with multi-stakeholder participation in power grid operation. To do this, a two-level optimization dispatching model between ADN and VMG based on the ATC method is proposed. A simulated case study is conducted to demonstrate the proposed model and its reliability and effectiveness are verified by various comparisons. Additionally, the following conclusions are drawn:

(1) The cooperative optimization dispatching of ADN and VMG can not only improve the reliability of power supply in the ADN but also improve the economics of ADN and VMG.

(2) By using the second-order cone programming to linearize the power flow calculation, the model solving's solving speed is improved.

(3) By adding the penalty function with the transmission variables to the ATC, the complete decoupling of the inter-region optimization problem is realized.

It should be noted that the reactive power output equipment in VMG is relatively single, PV and RL are output with constant power factor, and only DG has some flexibility in VMG reactive power optimization dispatching process. In addition, since this paper focuses on the economics of renewable energy, the uncertainty of its output is weakened. Therefore, in the follow-up research, it is necessary to further enrich the reactive power output equipment of VMG and pay attention to the impact of renewable energy output uncertainty on model optimization results. Moreover, it would also be interesting to study the joint optimization dispatching problem between the active distribution network and the regional distribution network with multiple VMGs.

APPENDIX A
MODELING PRINCIPLE BASED ON ATC METHOD

If ADN and VMG are regarded as independent optimization subjects, and for ADN, let x be the optimization variable, then the optimization problem can be expressed as follows.

$$\begin{aligned} & Min\, f(x) \\ & s.t.\ g(x) \leq 0 \\ & \quad\quad h(x) = 0 \end{aligned} \tag{A-1}$$

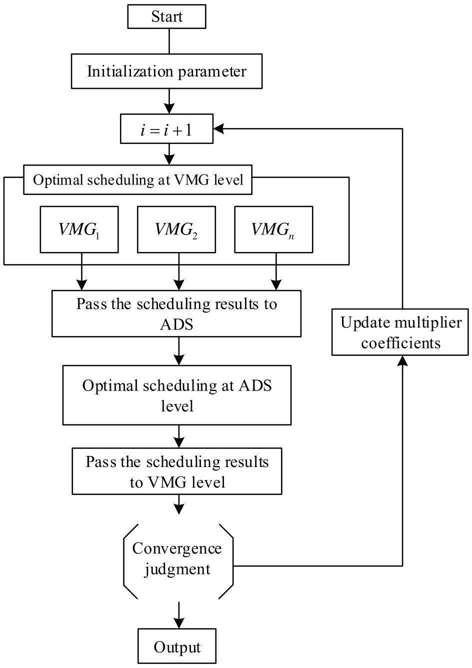

FIGURE 17. The solving process of bi-level optimal dispatching model.

For VMG_i, let y_i be the optimization variable, then the optimization problem can be expressed as follows.

$$\begin{aligned} &Min\, f\,(y_i) \\ &s.t.\; g\,(y_i) \le 0 \\ &\quad h\,(y_i) = 0 \end{aligned} \tag{A-2}$$

Considering that VMG_i and ADN are connected to each other and there is a coupling change between them, let x and y_i be the peculiar variables within their respective systems, and z be the coupling variables between them, then the ADN optimization problem can be re-expressed as follows.

$$\begin{aligned} &Min\, f\,(x, z_1, z_2, \ldots, z_n) \\ &s.t.\; g\,(x, z_1, z_2, \ldots, z_n) \le 0 \\ &\quad h\,(x, z_1, z_2, \ldots, z_n) = 0 \end{aligned} \tag{A-3}$$

The VMG_i optimization problem can be re-expressed as follows.

$$\begin{aligned} &Min\, f\,(y_i, z_i) \\ &s.t.\; g\,(y_i, z_i) \le 0 \\ &\quad h\,(y_i, z_i) = 0 \end{aligned} \tag{A-4}$$

Because of the existence of coupling variables, (A-3) and (A-4) cannot be solved independently. We define the active and reactive information transmitted from ADN to VMG_i as target variable, denoted by η, and the variable transmitted from VMG_i to ADN as the response variable, denoted by μ. The consistency constraint can be represented as follows.

$$c = \eta - \mu = 0 \tag{A-5}$$

The target variable and response variable essentially represent the same common variable, so this paper adds a penalty function to relax the algorithm. The penalty function is defined as $\pi\,(c)$.

Accordingly, the ADN optimization problem is replaced by the following model.

$$\begin{aligned} &Min\, f\,(x, \eta_1, \eta_2, \ldots, \eta_n) + \pi\,(c_1, c_2, \ldots, c_n) \\ &s.t.\; g\,(x, \eta_1, \eta_2, \ldots, \eta_n) \le 0 \\ &\quad h\,(x, \eta_1, \eta_2, \ldots, \eta_n) = 0 \end{aligned} \tag{A-6}$$

Moreover, the VMG_i optimization problem is replaced by the following model.

$$\begin{aligned} &Min\, f\,(y_i, \mu_i) + \pi\,(c_i) \\ &s.t.\; g\,(y_i, \mu_i) \le 0 \\ &\quad h\,(y_i, \mu_i) = 0 \end{aligned} \tag{A-7}$$

TABLE 6. Data statistics of ADN structure framework.

Starting node	Arrived at the node	R/pu	X/pu
1	2	0.01	0.04
2	3	0.03	0.68
3	4	0.04	0.12
4	5	0.06	0.17
5	6	0.03	0.09
6	7	0.09	0.25
7	8	0.03	0.08
8	9	0.17	0.21
9	10	0.41	0.31
4	11	0.17	0.22
3	12	0.29	0.38
12	13	0.22	0.29
13	14	0.48	0.62
13	15	0.40	0.52
15	16	0.29	0.38
15	17	0.37	0.46
17	18	0.11	0.14

TABLE 7. Typical daily load parameters and PV output parameters.

Time	Load	PV	Time	Load	PV
1	0.30	0	13	0.74	0.9
2	0.47	0	14	0.90	0.7
3	0.48	0	15	0.95	0.52
4	0.66	0	16	0.96	0.22
5	0.70	0	17	1.11	0.26
6	0.77	0.12	18	1.23	0.11
7	0.78	0.21	19	0.93	0
8	1.19	0.35	20	0.82	0
9	1.28	0.91	21	0.62	0
10	1.06	0.96	22	0.71	0
11	1.03	0.91	23	0.73	0
12	0.96	0.95	24	1.24	0

The coupling variables in this paper are the active power and reactive power transmitted between VMG and ADN, and the penalty function is an augmented Lagrange penalty function in the following form:

$$\pi\,(c) = v^T c + \|w \circ c\|^2 \tag{A-8}$$

TABLE 8. Operating parameters of VMG.

	parameter	value
DG_{VMG}	$P_{\max}^{VMG}$ / kW	600
	$P_{\max}^{ADN}$ / kW	1000
	a/b(￥/(kWh))	0.7
	Re	0.25
	η	0.5448t/MWh
	μ	0.5192
ESS	C_{ins}	3000yuan/kWh
	C_{eo}	0.054yuan/kWh
	L	20 year
	Charge discharge rate	0.938
	SOC_0	0.2
	$ESS_{\max}^{VMG}$ / kW	40
	$ESS_{\max}^{ADN}$ / kW	200
RL	C_{rl}	0.68yuan/kWh
PV	Pmax/kW	400
	Cost/yuan	0.6
	η	0.5192
CB	$N_i^{CB,\max}$	30
	$Q_{i,step}^{CB}$ / $kVar$	80
	$B_{CB}^{\lim}$	10

where v and w are the algorithm coefficient, $\circ$ represents itemized multiplication calculation. The ADN optimization problem can be finally expressed as follows.

$$\begin{aligned} & Min\, f\left(x, \eta_1, \eta_2, \ldots, \eta_n\right)+\sum_{t}^{T}\sum_{k=1}^{n}\left[\begin{array}{l} v_{k,t}\left(\eta_{i,t}-\overline{\mu_{i,t}}\right) \\ +\left(w_{k,t}\left(\eta_{i,t}-\overline{\mu_{i,t}}\right)\right)^2 \end{array}\right] \\ & s.t.\ g\left(x, \eta_1, \eta_2, \ldots, \eta_n\right) \leq 0 \\ & \quad h\left(x, \eta_1, \eta_2, \ldots, \eta_n\right)=0 \end{aligned} \tag{A-9}$$

Similarly, the VMG_i optimization problem can be finally expressed as follows.

$$\begin{aligned} & Min\, f\left(y_i, \mu_i\right)+\sum_{t}^{T}\left[v_{i,t}\left(\overline{\eta_{i,t}}-\mu_{i,t}\right)+\left(w_{i,t}\left(\overline{\eta_{i,t}}-\mu_{i,t}\right)\right)^2\right] \\ & s.t.\ g\left(y_i, \mu_i\right) \leq 0 \\ & \quad h\left(y_i, \mu_i\right)=0 \end{aligned} \tag{A-10}$$

where η and μ are respectively represented as follows.

$$\mu=\left[\begin{array}{l} P_{low} \\ Q_{low} \end{array}\right] \quad \eta=\left[\begin{array}{l} P_{up} \\ Q_{up} \end{array}\right]$$

After decomposing the solution process of the above problem, the optimization model of each level system can be obtained, and the iterative solution can be carried out according to the optimization flow chart shown in Figure 3.

APPENDIX B
STUDY PARAMETER

See Table 6, 7, 8.

REFERENCES

[1] K. Meng, Z. Y. Dong, Z. Xu, Y. Zheng, and D. J. Hill, "Coordinated dispatch of virtual energy storage systems in smart distribution networks for loading management," *IEEE Trans. Syst., Man, Cybern., Syst.*, vol. 49, no. 4, pp. 776–786, Apr. 2019.

[2] F. Wang, H. Xu, T. Xu, K. Li, M. Shafie-Khah, and J. P. Catalão, "The values of market-based demand response on improving power system reliability under extreme circumstances," *Appl. Energy*, vol. 193, pp. 220–231, May 2017.

[3] Q. Chen, F. Wang, B.-M. Hodge, J. Zhang, Z. Li, M. Shafie-Khah, J. P. S. Catalão, "Dynamic price vector formation model-based automatic demand response strategy for PV-assisted EV charging stations," *IEEE Trans. Smart Grid*, vol. 8, no. 6, pp. 2903–2915, Nov. 2017.

[4] S. Talari, M. Shafie-khah, F. Wang, J. Aghaei, and J. P. S. Catalão, "Optimal scheduling of demand response in pre-emptive markets based on stochastic bilevel programming method," *IEEE Trans. Ind. Electron.*, vol. 66, no. 2, pp. 1453–1464, Feb. 2019.

[5] F. Wang, K. Li, C. Liu, Z. Mi, M. Shafie-Khah, and J. P. S. Catalão, "Synchronous pattern matching principle-based residential demand response baseline estimation: Mechanism analysis and approach description," *IEEE Trans. Smart Grid*, vol. 9, no. 6, pp. 6972–6985, Nov. 2018.

[6] F. Wang, L. Zhou, H. Ren, X. Liu, M. Shafie-Khah, and J. P. S. Catalão, "Multi-objective optimization model of source-load-storage synergetic dispatch for a building energy management system based on TOU price demand response," *IEEE Trans. Ind. Appl.*, vol. 54, no. 2, pp. 1017–1028, Mar./Apr. 2018.

[7] F. Kamyab, M. Amini, S. Sheykhha, M. Hasanpour, and M. M. Jalali, "Demand response program in smart grid using supply function bidding mechanism," *IEEE Trans. Smart Grid*, vol. 7, no. 3, pp. 1277–1284, May 2016.

[8] J. Lu, W. Chu, H. Ren, T. He, and F. Wang, "Coordinated optimal dispatch of multi-stakeholder game based on demand response for active distribution network," *IET Renew. Power Gener.*, vol. 13, no. 6, pp. 898–904, 2019.

[9] R. Li, W. Wang, X. Z. Wu, F. Tang, and Z. Chen, "Cooperative planning model of renewable energy sources and energy storage units in active distribution systems: A bi-level model and Pareto analysis," *Energy*, vol. 168, pp. 30–42, Feb. 2019.

[10] Q. Y. Guo, K. J. Wu, M. Chao, and H. H. Xu, "A model for multi-objective coordination optimization of voltage and reactive power in distribution networks based on mixed integer second-order cone programming," *J. Electr. Eng. China*, vol. 38, no. 5, pp. 1385–1396, 2018.

[11] J. Zhu, Y. Yuan, and W. Wang, "Multi-stage active management of renewable-rich power distribution network to promote the renewable energy consumption and mitigate the system uncertainty," *Int. J. Elect. Power Energy Syst.*, vol. 111, pp. 436–446, Oct. 2019.

[12] S. Golshannavaz, S. Afsharnia, and P. Siano, "A comprehensive stochastic energy management system in reconfigurable microgrids," *Int. J. Energy Res.*, vol. 40, no. 11, pp. 1518–1531, 2016.

[13] H. Yuhui, L. Dong, and L. Huaiqing, "Site and size selection strategies of energy storage system based on power supply and storage capability index," in *Proc. Int. Conf. Renew. Power Gener.*, 2016, p. 6.

[14] M. Mazidi, H. Monsef, and P. Siano, "Incorporating price-responsive customers in day-ahead scheduling of smart distribution networks," *Energy Convers. Manage.*, vol. 115, pp. 103–116, May 2016.

[15] W. Wei, F. Liu, and S. Mei, "Energy pricing and dispatch for smart grid retailers under demand response and market price uncertainty," *IEEE Trans. Smart Grid*, vol. 6, no. 3, pp. 1364–1374, May 2015.

[16] X. Bai, W. Qiao, H. Wei, F. Huang, and Y. Chen, "Bidirectional coordinating dispatch of large-scale V2G in a future smart grid using complementarity optimization," *Int. J. Elect. Power Energy Syst.*, vol. 68, pp. 269–277, Jun. 2015.

[17] M. Shafiekhani, A. Badri, M. Shafie-khah, and J. P. S. Catalão, "Strategic bidding of virtual power plant in energy markets: A bi-level multi-objective approach," *Int. J. Elect. Power Energy Syst.*, vol. 113, pp. 208–219, Dec. 2019.

[18] M. Saffari, M. S. Misaghian, M. Kia, A. Heidari, D. Zhang, P. Dehghanian, and J. Aghaei, "Stochastic robust optimization for smart grid considering various arbitrage opportunities," *Electr. Power Syst. Res.*, vol. 174, Sep. 2019, Art. no. 105847.

[19] X. Wang, Z. Y. He, and J. W. Yang, "Unified strategy for electric vehicles participate in voltage and frequency regulation with active power in city grid," *IET Gener. Transmiss. Distrib.*, vol. 13, no. 15, pp. 3281–3291, 2019.

[20] H. Yang, D. Yi, J. Zhao, F. Luo, and Z. Dong, "Distributed optimal dispatch of virtual power plant based on ELM transformation," *J. Ind. Manage. Optim.*, vol. 10, no. 4, pp. 1297–1318, 2014.
[21] S. Ganguly, N. C. Sahoo, and D. Das, "Mono- and multi-objective planning of electrical distribution networks using particle swarm optimization," *Appl. Soft Comput.*, vol. 11, no. 2, pp. 2391–2405, 2011.
[22] P. Grošelj and L. Z. Stirn, "Evaluation of several approaches for deriving weights in fuzzy group analytic hierarchy process," *J. Decis. Syst.*, vol. 27, pp. 217–226, Apr. 2018.
[23] T. Sattarpour, S. Golshannavaz, D. Nazarpour, and P. Siano, "A multi-stage linearized interactive operation model of smart distribution grid with residential microgrids," *Int. J. Elect. Power Energy Syst.*, vol. 108, pp. 456–471, 2019.
[24] M. E. Baran and F. F. Wu, "Network reconfiguration in distribution systems for loss reduction and load balancing," *IEEE Trans. Power Del.*, vol. 4, no. 2, pp. 1401–1407, Apr. 1989.
[25] Z. Miao, L. Fan, H. G. Aghamolki, and B. Zeng, "Least squares estimation based SDP cuts for SOCP relaxation of AC OPF," *IEEE Trans. Autom. Control*, vol. 63, no. 1, pp. 241–248, Jan. 2018.
[26] E. D. Andersen, C. Roos, and T. Terlaky, "On implementing a primal-dual interior-point method for conic quadratic optimization," *Math. Program.*, vol. 95, no. 2, pp. 249–277, 2003.
[27] Y. Liu, W. Wu, B. Zhang, Z. Li, and Z. Li, "A mixed integer second-order cone programming based active and reactive power coordinated multi-period optimization for active distribution network," *Proc. CSEE*, vol. 34, no. 16, pp. 2575–2583,2014.
[28] Y. Fu and M. Shahidehpour, "Fast SCUC for large-scale power systems," *IEEE Trans. Power Syst.*, vol. 22, no. 4, pp. 2144–2151, Nov. 2007.
[29] A. Kalantari, J. F. Restrepo, and F. D. Galiana, "Security-constrained unit commitment with uncertain wind generation: The loadability set approach," *IEEE Trans. Power Syst.*, vol. 28, no. 2, pp. 1787–1796, May 2013.
[30] A. Kargarian and Y. Fu, "System of systems based security-constrained unit commitment incorporating active distribution grids," *IEEE Trans. Power Syst.*, vol. 29, no. 5, pp. 2489–2498, Sep. 2014.
[31] M. Zhou, J. Zhai, G. Li, and J. Ren, "Distributed dispatch approach for bulk AC/DC hybrid systems with high wind power penetration," *IEEE Trans. Power Syst.*, vol. 33, no. 3, pp. 3325–3336, May 2018.
[32] N. Michelena, H. Park, and P. Y. Papalambros, "Convergence properties of analytical target cascading," *AIAA J.*, vol. 41, no. 5, pp. 897–905, 2012.
[33] J. Lofberg, "YALMIP: A toolbox for modeling and optimization in MATLAB," in *Proc. IEEE Int. Conf. Robot. Automat.*, Sep. 2004, pp. 284–289.
[34] R. Li, W. Wang, and M. Xia, "Cooperative planning of active distribution system with renewable energy sources and energy storage systems," *IEEE Access*, vol. 6, pp. 5916–5926, 2018.

PULIANG DU received the M.S. degree from the School of Information and Electrical Engineering, China University of Taiyuan University of Technology, in 2017. He is currently pursuing the Ph.D. degree with the School of Electrical Engineering, Southeast University, China. His research interests include the optimal dispatching of the distribution networks and integrated power system operation and control.

ZHONG CHEN received the M.S. and Ph.D. degrees from the School of Electrical Engineering, Southeast University, China, in 2002 and 2006, respectively. He is currently a Full Professor with the Electrical Engineering School, Southeast University. His research interests include electric vehicles, renewable energy, and integrated power system operation and control.

YANXI CHEN received the B.E. degree in electrical engineering from the Dalian University of Technology, Dalian, China, in 2018. She is currently pursuing the master's degree with the School of Electrical Engineering, Southeast University, China. Her research interest includes the charging transaction of electric vehicles.

ZIWEN MA received the B.S. degree from the College of Electrical Engineering, Wuhan University, China, in 2016. He is currently pursuing the master's degree with the School of Electrical Engineering, Southeast University, China. His research interest includes the integration of electric vehicles into the modern power systems.

HONGEN DING received the M.S. degree from the School of Information and Electrical Engineering, China University of Southeast University. His main research interests include the technologies of power grid dispatching automation and intellectualization.